Fluctuations in photoionization cross sections of singlet planar helium

Johannes Eiglsperger and Javier Madroñero
Physik Department, Technische Universität München, DE-85747 Garching, Germany
(Received 30 December 2009; published 23 September 2010)

The fluctuating part of the total photoionization cross sections up to the 20th single ionization threshold from the ground state of helium are investigated within a planar model of the atom. The calculated fluctuations reproduce existing experimental observations rather well. The fluctuations are mainly due to a dominant series of resonances which can be associated with an approximate quantum number $F = N - K$. As the energy approaches the double ionization threshold, the dominant role of a single series as sole contributor is apparently lost as new series start to contribute significantly to the cross sections.

DOI: 10.1103/PhysRevA.82.033422 PACS number(s): 32.80.Fb, 31.15.A−, 32.30.−r

I. INTRODUCTION

Despite the seemingly simple problem of three charged particles with known interactions, there exists no comprehensive understanding of highly doubly excited states of two-electron atoms. As compared with hydrogen, helium contains the electron-electron interaction which is responsible for the complex classical dynamics [1,2]. On the quantum level, the spectrum of the semiclassical regime of highly doubly excited states is expected to be influenced by the underlying classical chaotic dynamics; and typical signatures of quantum chaos, such as a Wigner distribution of the energy spacings between nearest-neighbor resonances [3], semiclassical scaling laws for the fluctuations in the spectrum close to the double ionization threshold [4], or Ericson fluctuations [5–7], are expected to become observable [8].

Doubly excited states of two-electron atoms are organized in series converging toward the single ionization thresholds (SITs) I_N of He$(N)^+$ states. Starting from the fourth SIT, members of higher lying series interfere with lower series. Above the eighth ionization series, the widths of the resonances can be larger than their separation [9,10]. Close to the double ionization threshold (DIT), the density of states increases significantly. As a consequence, it has long been speculated about the existence and onset of the Ericson regime of strongly overlapping autoionizing states. Also, the number of open channels increases dramatically approaching the DIT. Therefore, an accurate treatment of this problem defines a theoretical and numerical challenge. Studies on quantum chaos of the one-dimensional (1D) helium atom have predicted Ericson fluctuations in the total photoionization cross sections (TPCS) to be observable above I_{34} [11,12], and studies within the s^2 model find Ericson fluctuations in the partial inelastic cross sections between electrons and He^+ already around I_{16} [13]. Currently available full three-dimensional (3D) approaches are able to describe the spectrum up to the $N = 17$ threshold [12]. The analysis of the theoretical and experimental results up to $I_{N=17}$ in [12] reveals a clear dominance of principal Rydberg series in the total photoionization cross section. These series are associated with the approximate quantum number $F = N - K$ given in terms of the inner electron excitation N and the parabolic quantum number K of Herrick's algebraic classification [14–16]. Consequently, Ericson fluctuations are absent in this regime in clear contradiction with the predictions of simplified models [13].

In a recent paper [17], we investigated the fluctuations in the TPCS in the energy regime up to I_{20} of triplet planar (2D) helium. In addition to the existence of dominant series in the TPCS and of the approximate quantum number F for a large fraction of the resonances, we observed also a competition in the contributions between the dominant and subdominant series at high energies which eventually could lead to an earlier onset of Ericson fluctuations. The relevance of this competition for the real atom is shown in this article, where we explore the fluctuations in the TPCS from the ground state of singlet planar helium into the resonances up to the 20th ionization threshold and reproduce the observations by Jiang *et al.* [4].

The paper is organized as follows. In Sec. II, we outline our theoretical and numerical setup. Section III provides a description of the spectral properties of planar helium up to the 20th ionization threshold, and discusses the role of Rydberg series associated with the low-dimensional eZe configuration in the TPCS. Section IV concludes the paper. Unless stated otherwise, atomic units are used throughout this document. For the conversion, 1 a.u. = 27.211 389 5 eV has been used.

II. THEORY AND NUMERICAL IMPLEMENTATION

A detailed description of our approach for planar helium has already been presented elsewhere [17–20]. We will thus give only a brief review of its most relevant aspects.

The Hamiltonian describing the helium atom, in atomic units, reads as

$$H = \frac{\vec{p}_1^{\,2} + \vec{p}_2^{\,2}}{2} - \frac{Z}{r_1} - \frac{Z}{r_2} + \frac{1}{r_{12}}\,, \tag{1}$$

where $\vec{p}_i$ and r_i, $i = 1,2$, denote the respective momenta and positions of both electrons, r_{12} represents the interelectronic distance, the nucleus (with infinite mass) is fixed at the origin, and Z is the nuclear charge. The classical dynamics generated by this Hamiltonian is invariant with respect to the energy E of the two-electron system [19–21]. In particular, the angular momentum scales as $L^{\rm sc} = |E|^{\frac{1}{2}} L$. Therefore, for moderate values of L and highly doubly excited states ($E \simeq 0$), the scaled angular momentum is close to zero, tantamount to an almost planar three-body configuration. Precisely this is the semiclassical energy regime in which one expects that classical and quantum dynamics are similar. From now on we restrict our problem to two dimensions, i.e., the electrons and the

nucleus are confined to a plane. In this case, two successive, parabolic coordinate transformations and a suitable rotation completely regularize all singularities in the Hamiltonian and finally allow one to identify the eigenvalue problem generated by (1) with an eigenvalue problem describing *four* coupled harmonic oscillators [18–20]. Consequently, (1) can be represented in a basis set defined by the tensor product

$$|n_1 n_2 n_3 n_4\rangle = |n_1\rangle \otimes |n_2\rangle \otimes |n_3\rangle \otimes |n_4\rangle \tag{2}$$

of Fock states of the individual harmonic oscillators, and has a purely algebraic representation in the associated annihilation and creation operators that define the four-oscillator algebra. This representation leads to a generalized eigenvalue problem which involves polynomials of maximal degree 16 in the creation and annihilation operators, with altogether 1511 monomial terms, and thus allows a purely analytical calculation of all matrix elements defining our eigenvalue problem [19,20]. The Hamiltonian (1) is invariant under the particle exchange symmetry P_{12} and the symmetry Π_x with respect to the x axis. It also commutes with the total angular momentum l. This leads to a reduction of the eigenvalue problem.

The resolution of the resonances in the complex plane is achieved with the help of the complex rotation method [22–26], consisting of a rotation of the coordinates by a suitable angle θ into the complex plane. In addition to this, we also introduce a dilation of the coordinates by a real parameter α. The complex dilation is thus achieved through the transformations $\vec{r} \to \alpha \vec{r} \exp(i\theta)$ and $\vec{p} \to \vec{p} \exp(-i\theta)/\alpha$. Though the dilation by α is a unitary transformation, the whole transformation leads to a complex symmetric matrix representation of the generalized eigenvalue problem. Its spectrum is complex in general with the following properties:

(a) The bound states of the Hamiltonian (1) are invariant under complex rotation.

(b) There are isolated complex eigenvalues $E_{i,\theta} = E_i - i\Gamma_i/2$ in the lower half plane, corresponding to resonance states. These are stationary under changes of θ, provided the dilation angle is large enough to uncover their positions on the Riemannian sheets of the associated resolvent [27,28]. The associated resonance eigenfunctions are square integrable [29], in contrast to the resonance eigenfunctions of the unrotated Hamiltonian.

(c) The continuum states are located on half lines, rotated by an angle -2θ around the ionization thresholds of the unrotated Hamiltonian, into the lower half of the complex plane.

Due to the polynomial character of the representation in creation and annihilation operators, these complex symmetric matrices have a sparse banded structure with 159 coupling matrix elements in the band. The basis $|n_1 n_2 n_3 n_4\rangle$ is properly symmetrized and truncated for numerical implementation. The description of highly doubly excited states requires the diagonalization of a generalized eigenvalue problem involving matrices of typically large dimensions (e.g., 394161×18498 for $\max(n_1,n_2,n_3,n_4) = 420$ for the description of singlet P states around the 20th ionization threshold). This is achieved with the help of an efficient implementation of the Lanczos algorithm [30–32], which uses advanced techniques of parallel programming [33,34]. The numerical diagonalization was carried out on large computers like the HLRB II of the Bayerische Akademie der Wissenschaften [35].

The photoionization cross section can be calculated in terms of the eigenvalues $E_{i,\theta}$ and eigenstates $|\psi_{i,\theta}\rangle$ of the complex rotated Hamiltonian. The photoionization cross section from the initial state $|\phi_E^{\text{in}}\rangle$ with energy E_{in} into the final states mediated by a photon with energy ω is given by

$$\sigma(\omega) = \frac{4\pi\omega}{c} \text{Im}\left[\sum_i \frac{\langle\overline{\psi_{i,\theta}}|R(\theta)T|\phi_E^{\text{in}}\rangle^2}{E_{i,\theta} - E_{\text{in}} - \omega}\right], \tag{3}$$

where $T = \vec{e}\cdot\vec{r}$ is the dipole operator with the light polarization $\vec{e}$, $\langle\overline{\psi_{i,\theta}}|$ is the transpose of $|\psi_{i,\theta}\rangle$ in the representation described above, and $R(\theta) = \exp[-\theta(\vec{r}\cdot\vec{p} + \vec{p}\cdot\vec{r})/2]$ is the complex rotation operator. Transformation into the appropriate coordinates allows one to represent the matrix elements of the dipole operator in the creation and annihilation operators. The sum in Eq. (3) includes all eigenvalues and eigenstates of the rotated Hamiltonian. The continuum states are responsible for the smooth background σ_{bg} of the cross sections, which is the average of the cross sections. The fluctuating part $\sigma_{\text{fl}} = \sigma - \sigma_{\text{bg}}$ of the cross sections—which is dominated by Fano profiles for low energies or by a strong fluctuating pattern as the energy approaches the DIT—is determined by the resonances. Therefore, in order to numerically calculate the fluctuating part σ_{fl} of the TPCS, only resonances are plugged into Eq. (3).

Further insight into the spectral structure and important features of the underlying classical dynamics are obtained through the expectation value for each resonance state of the cosine of the angle θ_{12} between the electron positions $\vec{r}_1$ and $\vec{r}_2$ ($\langle\cos\theta_{12}\rangle$). The operator $\cos\theta_{12}$ has also an exact polynomial representation in terms of the creation and annihilation operators, and its expectation value for a given state $|\psi_i\rangle$ in terms of the rotated states is [17]

$$\langle\psi_i|\cos\theta_{12}|\psi_i\rangle \approx \text{Re}(\langle\overline{\psi_{i,\theta}}|\cos\theta_{12}|\psi_{i,\theta}\rangle)\,. \tag{4}$$

III. RESULTS

As in the three-dimensional case [2], the eigenstates of 2D helium are organized in series converging to single ionization thresholds which all converge to the double ionization threshold at zero energy. The threshold structure of the spectrum is essentially the same as for the case without electron-electron interaction, and the location of the various single ionization thresholds is unaffected by the term $1/r_{12}$, since the electron-electron interaction vanishes at large distances. Thus, the Nth threshold energy is given by [18,19]

$$I_N = -\frac{2}{(N-1/2)^2}\ \text{a.u.}, \quad N \in \mathbb{N}, \tag{5}$$

a series which obviously converges to zero with $N \to \infty$. The first series of eigenenergies converges to the threshold $I_1 = -8$ a.u., and above this energy all bound states with $N > 1$ are embedded into the continuum of lower series; i.e., they are resonance states with finite width [28]. Due to the truncation of the basis, the exact thresholds cannot be reached, but only effective thresholds I_N^{eff} [33,36]. The spectrum can be classified by the particle exchange symmetry P_{12}, the symmetry Π_x with

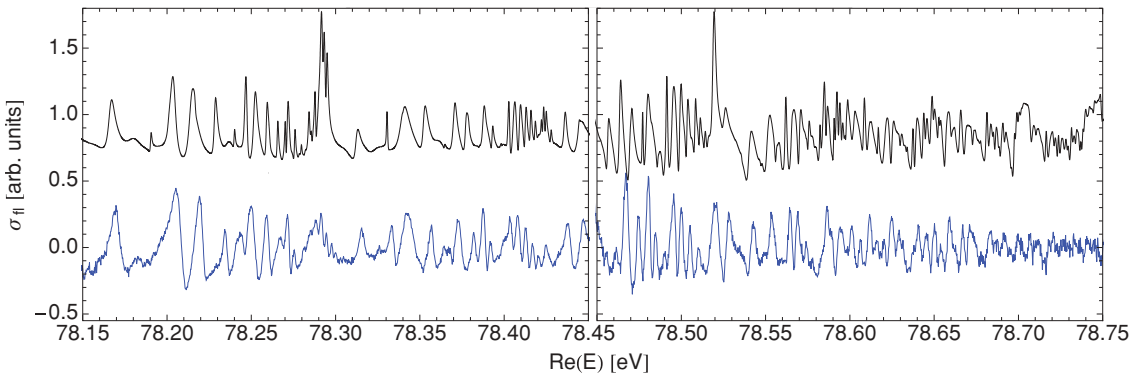

FIG. 1. (Color online) Fluctuations of the photoionization cross section of doubly excited singlet helium between I_8 and I_{15}: experimental data (bottom, blue) and theoretical results for planar helium (top, black). The theoretical data were scaled according to Eq. (8) and afterward convoluted by a Gaussian function with 1.7 meV width (FWHM). For clarity, the theoretical data are displaced by −9 meV in horizontal direction and one unit in vertical direction. The amplitude of the cross section in the right panel has been enlarged by a factor of 2.5 with respect to the left panel.

respect to the x axis, and the absolute value $|l|$ of the angular momentum (or, equivalently, l^2).

In this work we investigate the photoionization cross section for dipole transitions from the singlet planar helium ground state, with angular momentum $l = 0$ and $\Pi_x = +1$. The energy of this state is given by

$$E_{\text{in}} = -11.899\,822\,342\,953\,0 \text{ a.u.} \tag{6}$$

The dipole operator couples this state with $|l| = 1$ singlet states of symmetry $\Pi_x = +1$. The resolution of the TPCS at high energies close to the double ionization threshold requires the accurate calculation of the spectrum associated with these states. The numerically obtained spectrum contains discretized continuum states rotated by 2θ in the complex plane, converged resonances (stable under moderate variations of α and θ), and numerical artifacts and nonconverged resonances (θ- and α-dependent) due to the truncation of the basis [17]. To extract the converged resonances, all data points have been checked for convergence with data for other parameter sets (α,θ). Depending on the energy regime, these parameters have to be adjusted. Finally, a given energy regime is calculated with 6–12 parameter sets (α,θ) among {(0.35,0.15), (0.35,0.20), (0.35,0.25), (0.35,0.30), (0.40,0.15), (0.40,0.20), (0.40,0.25), (0.40,0.30), (0.45,0.10), (0.45,0.15), (0.50,0.10), (0.50,0.15), (0.50,0.20), (0.50,0.25), (0.50,0.30), (0.55,0.10), (0.55,0.15)}. As the criterion of convergence for the resonances, we used a coincidence, for resonances of at least four different parameter sets (α,θ), within a maximal deviation of a factor of 10^{-5} for $\text{Re}(E_{i,\theta})$ (that is, a coincidence of five significant digits), 10^{-2} for $\text{Im}(E_{i,\theta})$, 10^{-2} for $\langle\cos\theta_{12}\rangle$, and 5×10^{-2} for $\langle\overline{\psi_{i,\theta}}|R(\theta)T|\phi_E^{\text{in}}\rangle^2$. In addition, we checked that the real part of $\langle\overline{\psi_{i,\theta}}|\cos\theta_{12}|\psi_{i,\theta}\rangle$ is at least two orders of magnitude larger than the imaginary part.

As the energy approaches the total breakup threshold, the density of states increases dramatically. Single resonances will overlap with other resonances in the sense that the widths of individual resonances are larger than the separation from their nearest-neighbor resonances. Individual Fano profiles are thus hard or impossible to distinguish, and the cross sections exhibit a strongly oscillating or fluctuating pattern around a smooth background. The fluctuating part $\sigma_{\text{fl}}(\omega)$ of the TPCS is given by Eq. (3), where only converged resonances are taken into account [17].

The TPCS for singlet planar helium from the ground state has been measured up to energies around the 15th SIT [12]. A direct comparison with the TPCS for planar helium is not possible, due to the different energy scales of the eigenstates of planar and 3D helium. In particular, the positions of the ionization thresholds for planar helium (5) do not coincide with those for the 3D system

$$I_N^{\text{3D}} = -\frac{2}{N^2}\,. \tag{7}$$

This problem can be solved by rescaling the energies for planar helium according to

$$E_{\text{2D}}^{\text{scaled}} = -\frac{2}{\left(\sqrt{-\frac{2}{E_{\text{2D}}}}+\frac{1}{2}\right)^2}\,. \tag{8}$$

In Fig. 1, energy-rescaled calculated fluctuations σ_{fl} for singlet planar helium are presented together with the experimental photoionization-yield spectra of doubly excited singlet helium from [12]. The energies are converted to eV (zero value fixed at the ground-state energy), and the calculated cross section has been convoluted by a Gaussian function with 1.7 meV [full width at half maximum (FWHM)], which is consistent with the experimental resolution. Our theoretical predictions have been slightly shifted by −0.009 eV in order to match the experiment.

Planar helium is known to provide a good qualitative description [37]. Figure 1 shows, moreover, the quantitative power of the planar approach. Characteristic features of the cross section are well resolved within the data by the planar model. Furthermore, experimental and theoretical data show excellent agreement concerning peak positions and peak shapes. Discrepancies seem to occur near the effective ionization thresholds. These observations support once again the expectation that the planar model describes helium for the energy regime close to the DIT rather well.

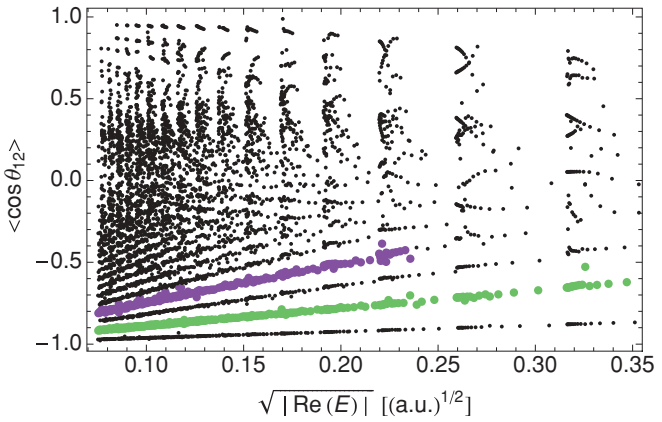

FIG. 2. (Color online) Calculated $\langle\cos\theta_{12}\rangle$ values as a function of resonance energy E below the 20th threshold. Each point represents a particular singlet state resonance with $\Pi_x = +1$ and $|l| = 1$. For values of $\langle\cos\theta_{12}\rangle$ close to -1, the resonances are organized in series along straight lines converging to -1 at the DIT. These series are labeled by the approximate quantum number F. The dominant and subdominant series are highlighted in color online: green (light gray) $F = 2$, purple (dark gray) $F = 4$.

The investigations by Jiang *et al.* [12,38] show that the total cross section is dominated by the low-dimensional collinear eZe dynamics. Only very few resonances contribute significantly to the photoionization cross section in the region from I_9 to I_{16}, and the series of contributing resonances are associated with (small) constant values of $F = N - K$, where N and K are approximate quantum numbers from Herrick's algebraic classification [14,15]. These observations have been verified up to the 20th SIT for triplet helium under a planar approach [17], where we predicted in addition a competition of the contributions to the TPCS of series associated with the values of $F = 1$, 3, and 5. In the rest of this section, we show that there is also a competition between different series in singlet helium.

Figure 2 presents a plot of the calculated expectation values $\langle\cos\theta_{12}\rangle$ as a function of $\sqrt{|\mathrm{Re}(E_\theta)|}$ for all converged resonances below I_4 up to I_{20}. θ_{12} is the angle between the two electron position vectors $\vec{r}_1$ and $\vec{r}_2$. A clear decomposition into series of resonances can be identified for $\langle\cos\theta_{12}\rangle \lesssim -0.5$. From the relation

$$\langle\cos\theta_{12}\rangle \overset{n\to\infty}{\longrightarrow} -\frac{K}{N}, \tag{9}$$

the eZe configuration can be identified with the maximum value of $K = N - 1$, i.e., $F = N - K = 1$.[1] Furthermore, the values of $\langle\cos\theta_{12}\rangle$ in the low-lying series in Fig. 2 decrease smoothly with decreasing values of $\sqrt{|\mathrm{Re}(E_\theta)|}$. This can be understood as a consequence of the presence of perturbers with different K values that belong to Rydberg series below the next higher thresholds, i.e., of a strong mixing of resonances with different N and K, but the same $N - K$. The approximate quantum number $F = N - K$ thus allows the classification of these series of resonances, of which all members lie on straight lines. As the energy approaches the DIT, new series associated with higher values of F appear, and no mixing between series with different values of F is found. In addition, the extrapolations of the straight lines for series classified by a constant value of F cross each other at a value of $\langle\cos\theta_{12}\rangle = -1$ at the DIT. In this limit, these resonances correspond to the eZe configuration, which is stable under angular perturbations, but unstable under radial perturbations. Therefore, the existence of the approximate quantum number F can be understood by the regularity in the angular direction in helium, though the radial motion remains chaotic. In contrast to these resonances, a series of resonances in the region where $\langle\cos\theta_{12}\rangle$ is close to $+1$ exhibits a systematic increase of $\langle\cos\theta_{12}\rangle$, though no mixing between N and K takes place. This is a consequence of the underlying regular classical dynamics of the frozen planet (Zee) configuration.

The approximate classification of helium resonances unveiled in Fig. 2 allows us to study separately the contributions of different series to the photoionization cross sections. Indeed, only a small fraction of states contribute significantly to the cross section. In contrast to triplet helium, for singlet states, the resonances which yield major contributions are characterized by even values of F,

$$F = 2m\,, \quad m \in \mathbb{N}\,, \tag{10}$$

which is a consequence of the propensity rules for dipole transitions [40]. Series with odd F and all resonances that cannot be characterized by F, e.g., those resonances close to the DIT for which $-0.5 \lesssim \langle\cos\theta_{12}\rangle$, result in almost no contribution.

In Fig. 3, we compare the fluctuations of the photoionization cross section with the contributions of the resonances associated with $F = 2$. The subset of resonances with $F = 2$ resembles the cross section quite well, and therefore it yields the dominant contributions. However, as the energy approaches the DIT, the influence of series with higher values of F grows. This is illustrated in Fig. 4, where we present the separate contributions of the series with $F = 2$ and $F = 4$, and the contributions of the remaining resonances. A direct

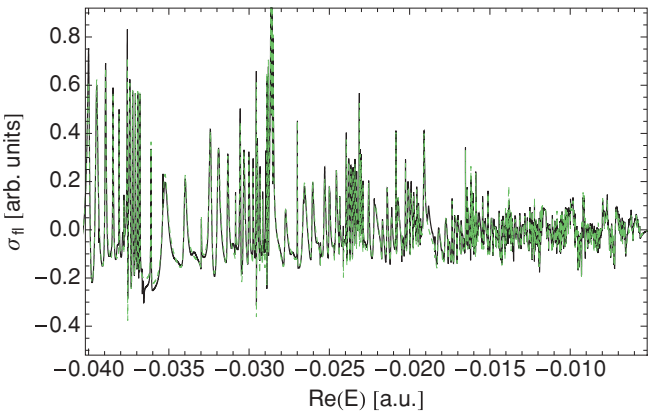

FIG. 3. (Color online) Comparison of the fluctuations of the photoionization cross sections from below I_8 up to I_{20} including all resonances (solid line) and resonances with $F = 2$ only (dashed line).

[1]Notice that Herrick's classification is also valid for the 2D model of helium. In this case, the quantum number T takes the value $T = 0$ [37,39].

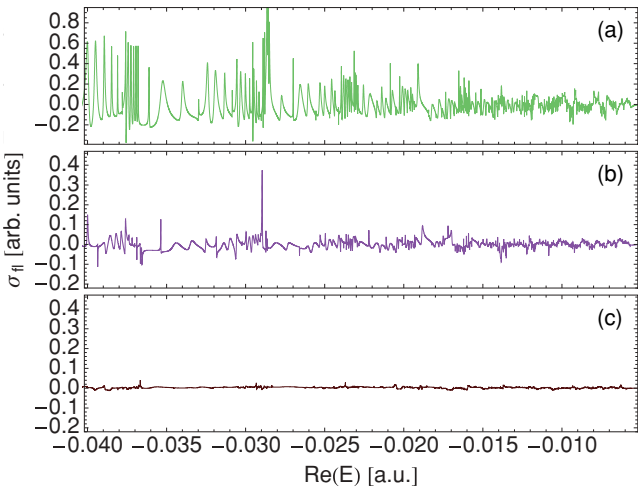

FIG. 4. (Color online) Contributions of subsets of resonances to the fluctuations of the photoionization cross section from below I_8 to below I_{20}. The fluctuations due to the series $F = 2$ and $F = 4$ are shown in (a) and (b), respectively. The contributions from all remaining resonances are depicted in (c). The rapid decrease of the amplitudes in (a) in comparison to (b) suggests a competition between the $F = 2$ and $F = 4$ series and an eventual loss of the dominant role of the $F = 2$ series.

comparison of the plots in Fig. 4 provides a rough estimate of the amplitudes of the fluctuations. The typical magnitude of the fluctuations for the resonances series $F = 2$ around I_9 is about six times larger than the one for the $F = 4$, which, however, reduces to a factor of roughly 2.5 around I_{18}. This might eventually lead to a breakdown of the dominant series picture and, therefore, to an earlier onset for a regime of strong overlapping of contributing resonances. In such a case, the peaks in the TPCS could not necessarily be associated with individual resonances. This is the scenario described in the seminal article by Ericson [5]; however, it is not yet found in helium below I_{20}. Indeed, it is possible to associate a single resonance of the $F = 2$ or $F = 4$ series with almost every peak in the cross section.

IV. SUMMARY AND CONCLUSIONS

A planar model for the helium atom has allowed the description of the spectrum of singlet states up to the 20th ionization threshold. Close to the DIT, the TPCS consists of a smooth background and a fluctuating part which is obtained from the resonances of the system. Within our approach, we have verified the existence of the approximate quantum number $F = N - K$ found by Jiang *et al.* [4] and of a dominant series in the TPCS associated with $F = 2$. Furthermore, we have shown that the relative weight of the contributions coming from the series with $F = 2$ and $F = 4$ changes with increasing energy and might break the dominance of the $F = 2$ completely at even higher energies. The existence of dominant series plays a fundamental role in the discussion about the existence of Ericson fluctuations in helium. The density of states reduces considerably after the restriction to the dominant series. The contributing resonances are practically isolated, in contrast to the strong overlapping exhibited by all resonances. Therefore, almost all peaks of the cross section can be identified with single resonances.

At high energies, the planar model is not only a tool for a qualitative description of the system. We have shown that the planar model can reproduce existing experimental observations and, therefore, it allows a quantitative description of helium. The investigations carried out for singlet helium here and for triplet helium in a previous work [17] acquire thus a new quality.

ACKNOWLEDGMENTS

We thank Yuhai Jiang and Ralph Püttner for sharing their experimental data with us, and we are indebted to Harald Friedrich and Moritz Schönwetter for enlightening discussions. Access to the computing facilities of the "Leibniz-Rechenzentrum der Bayerischen Akademie der Wissenschaft", as well as financial support by Deutsche Forschungsgemeinschaft under the Contract No. FR 591/16-1 are gratefully acknowledged.

[1] K. Richter, G. Tanner, and D. Wintgen, Phys. Rev. A **48**, 4182 (1993).
[2] G. Tanner, K. Richter, and J.-M. Rost, Rev. Mod. Phys. **72**, 497 (2000).
[3] O. Bohigas, M. J. Giannoni, and C. Schmit, Phys. Rev. Lett. **52**, 1 (1984).
[4] C. W. Byun, N. N. Choi, M.-H. Lee, and G. Tanner, Phys. Rev. Lett. **98**, 113001 (2007).
[5] T. Ericson, Phys. Rev. Lett. **5**, 430 (1960).
[6] T. Ericson, Ann. Phys. (NY) **23**, 390 (1963).
[7] J. Madroñero and A. Buchleitner, Phys. Rev. Lett. **95**, 263601 (2005).
[8] R. Blümel, Phys. Rev. A **54**, 5420 (1996).
[9] B. Grémaud and D. Delande, Europhys. Lett. **40**, 363 (1997).
[10] A. Czasch *et al.*, Phys. Rev. Lett. **95**, 243003 (2005).
[11] R. Blümel and W. P. Reinhardt, *Chaos in Atomic Physics* (Cambridge University Press, Cambridge, England, 1997).
[12] Y. H. Jiang, R. Püttner, D. Delande, M. Martins, and G. Kaindl, Phys. Rev. A **78**, 021401(R) (2008).
[13] J. Xu, A.-T. Le, T. Morishita, and C. D. Lin, Phys. Rev. A **78**, 012701 (2008).
[14] O. Sinanoglu and D. R. Herrick, J. Chem. Phys. **62**, 886 (1975).
[15] D. R. Herrick and O. Sinanoğlu, Phys. Rev. A **11**, 97 (1975).
[16] D. R. Herrick, Adv. Chem. Phys. **52**, 1 (1983).
[17] J. Eiglsperger and J. Madroñero, Phys. Rev. A **80**, 022512 (2009); **80**, 039902(E) (2009).
[18] L. Hilico, B. Grémaud, T. Jonckheere, N. Billy, and D. Delande, Phys. Rev. A **66**, 022101 (2002).
[19] J. Madroñero, Dissertation, Ludwig-Maximilians-Universität München, 2004, [http://edoc.ub.uni-muenchen.de/archive/00002187].
[20] J. Madroñero and A. Buchleitner, Phys. Rev. A **77**, 053402 (2008).
[21] I. C. Percival, Proc. R. Soc. London A **353**, 289 (1977).

[22] J. Aguilar and J. M. Combes, Commun. Math. Phys. **22**, 269 (1971).
[23] E. Balslev and J. M. Combes, Commun. Math. Phys. **22**, 280 (1971).
[24] B. Simon, Ann. Math. **97**, 247 (1973).
[25] W. P. Reinhardt, Annu. Rev. Phys. Chem. **33**, 223 (1982).
[26] S. Graffi, V. Grecchi, and H. J. Silverstone, Ann. Inst. Henri Poincaré A **42**, 215 (1985).
[27] M. Pont and R. Shakeshaft, Phys. Rev. A **43**, 3764 (1991).
[28] M. Reed and B. Simon, *Methods of Modern Mathematical Physics, Vol. 4: Analysis of Operators* (Academic Press, New York, 1978).
[29] Y. Ho, Phys. Rep. **99**, 1 (1983).
[30] C. Lanczos, J. Res. Natl. Bur. Stand. **45**, 255 (1950).
[31] B. N. Parlett and D. S. Scott, Math. Comput. **33**, 217 (1979).
[32] T. Ericsson and A. Ruhe, Math. Comput. **35**, 1251 (1980).
[33] A. Krug, Dissertation, Ludwig-Maximilians-Universität München, 2001, [http://edoc.ub.uni-muenchen.de/archive/00000336].
[34] [http://www.mpi-forum.org/docs/docs.html].
[35] [http://www.lrz-muenchen.de/services/compute/hlrb/].
[36] A. Buchleitner, D. Delande, and J.-C. Gay, J. Opt. Soc. Am. B **12**, 505 (1995).
[37] J. Madroñero, P. Schlagheck, L. Hilico, B. Grémaud, D. Delande, and A. Buchleitner, Europhys. Lett. **70**, 183 (2005).
[38] Y. H. Jiang, Dissertation, Freie Universität Berlin, 2006, [http://www.diss.fu-berlin.de/2006/269].
[39] C. D. Lin, Phys. Rev. A **29**, 1019 (1984).
[40] J. M. Rost, K. Schulz, M. Domke, and G. Kaindl, J. Phys. B **30**, 4663 (1997).